CALCULATION OF PATH-EQUIVALENT STRAIN RANGES OF MULTIAXIAL NON-PROPORTIONAL HISTORIES USING THE MOMENT OF INERTIA METHOD

H. Wu[1)], M.A. Meggiolaro[2)], J.T.P. Castro[2)]

[1)] School of Aerospace Engineering and Applied Mechanics, Tongji University
Siping Road 1239, 200092, Shanghai, P.R. China
[2)] Department of Mechanical Engineering, Pontifical Catholic University of Rio de Janeiro
Rua Marquês de São Vicente 225 – Gávea, Rio de Janeiro, RJ, 22453-900, Brazil

ABSTRACT

The Moment Of Inertia (MOI) method has been proposed by the authors to solve some of the shortcomings of the convex-enclosure methods to calculate path-equivalent ranges and mean components of complex non-proportional (NP) multiaxial load histories. For general histories, the load path must first be represented in a 5D deviatoric stress space. Such a stress path is then assumed to be represented by a homogeneous wire with unit mass, whose center of mass (centroid) is used to estimate the location of the mean component of the load path. The mass moment of inertia (MOI) of this hypothetical wire with respect to its centroid is calculated, which gives a measure of how much the load path stretches away from its mean component. The path-equivalent range of the true stress path is finally calculated as a function of this MOI, which can then be applied to stress-based damage models to predict fatigue initiation lives. In this work, the MOI method is reviewed and applied to multiaxial NP strain paths, to find an equivalent strain (or shear strain) range, associated with each rainflow-counted load event, for low-cycle strain-based damage calculations. A MOI version for critical-plane models is presented, where a path-equivalent shear strain range is obtained based on the projected shear-shear strain history on each candidate plane, providing better damage predictions for materials that fail due to a single dominant crack.

KEYWORDS

Multiaxial fatigue; Path-equivalent ranges; Non-proportional loading; Critical-plane method.

INTRODUCTION

The Moment Of Inertia (MOI) method [1] is used to predict equivalent stresses or strains in non-proportional (NP) loading histories, for multiaxial fatigue damage calculations. In the MOI method, the stress or strain path in the deviatoric space is assumed to be represented by a homogeneous wire with unit mass, whose center of mass (centroid) estimates the location of the mean component. Then, the mass moment of inertia (MOI) of this hypothetical wire with respect to its centroid is calculated, giving a measure of how much the path stretches away from its mean component. The path-equivalent range of the true stress or strain path is finally calculated as a function of this MOI, which is a physically sound approximation, since paths with larger amplitudes would be associated with wider wires with increased MOI.

The MOI method has been applied to tension-torsion [2] and to general 6D load histories [3], following a fatigue damage calculation approach based on stress invariants. For 6D histories, the history must first be represented in a 5D deviatoric stress or strain space, using the 5D vectors $\vec{s}'$ and $\vec{e}'$, defined as

$$\begin{cases} \vec{s}' \equiv [\, s_1 \;\; s_2 \;\; s_3 \;\; s_4 \;\; s_5 \,]^T \text{ and } \vec{e}' \equiv [\, e_1 \;\; e_2 \;\; e_3 \;\; e_4 \;\; e_5 \,]^T \\ s_1 \equiv \sigma_x - \dfrac{\sigma_y + \sigma_z}{2}, \quad s_2 \equiv \dfrac{\sigma_y - \sigma_z}{2}\sqrt{3}, \quad s_3 \equiv \tau_{xy}\sqrt{3}, \quad s_4 \equiv \tau_{xz}\sqrt{3}, \quad s_5 \equiv \tau_{yz}\sqrt{3} \\ e_1 \equiv \varepsilon_x - \dfrac{\varepsilon_y + \varepsilon_z}{2}, \quad e_2 \equiv \dfrac{\varepsilon_y - \varepsilon_z}{2}\sqrt{3}, \quad e_3 \equiv \dfrac{\gamma_{xy}}{2}\sqrt{3}, \quad e_4 \equiv \dfrac{\gamma_{xz}}{2}\sqrt{3}, \quad e_5 \equiv \dfrac{\gamma_{yz}}{2}\sqrt{3} \end{cases} \tag{1}$$

These deviatoric stress and strain spaces are convenient because their Euclidean norms $|\vec{s}'|$ and $|\vec{e}'|/(1+\bar{\nu})$ are equal to the von Mises equivalent stresses and strains, where $\bar{\nu}$ is an effective Poisson ratio. For 2D tension-torsion histories with stress paths defined by the normal and shear components σ_x and τ_{xy}, then $\sigma_y = \sigma_z = \tau_{xz} = \tau_{yz} = 0$, while $\varepsilon_y = \varepsilon_z = -\bar{\nu} / \varepsilon_x$ and $\gamma_{xz} = \gamma_{yz} = 0$. In this case,

$$s_1 \equiv \sigma_x, \quad s_2 \equiv 0, \quad s_3 \equiv \tau_{xy}\sqrt{3}, \quad s_4 \equiv 0, \quad s_5 \equiv 0 \tag{2}$$

$$e_1 \equiv \varepsilon_x - \frac{\varepsilon_y + \varepsilon_z}{2} = \varepsilon_x \cdot (1+\bar{\nu}), \quad e_2 \equiv \frac{\varepsilon_y - \varepsilon_z}{2}\sqrt{3} = 0, \quad e_3 \equiv \frac{\gamma_{xy}}{2}\sqrt{3}, \quad e_4 = e_5 \equiv 0 \tag{3}$$

Since only s_1, s_3, e_1, and e_3 are not null, the stress or strain paths of such tension-torsion histories can be represented in the 2D deviatoric diagrams $s_1 \times s_3$ or $e_1 \times e_3$, see Fig. 1.

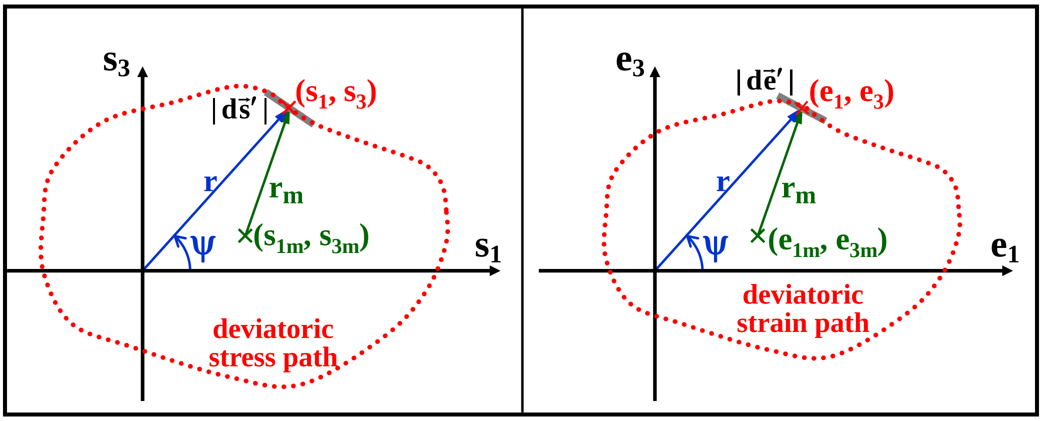

Fig. 1: Stress path of a 2D tension-torsion load history in a deviatoric stress diagram (left) and its corresponding strain path in a deviatoric strain diagram (right), both assumed as homogeneous wires with unit mass.

The tension-torsion version of the MOI method assumes that the 2D load path, which is represented by a series of points (s_1, s_3) or (e_1, e_3) that describe the stress or strain variations along it, is analogous to a homogeneous wire with unit mass. The mean component of the path is assumed to be located at the center of gravity of this hypothetical homogeneous wire shaped as the load history path. Its center of gravity is located at the perimeter centroid (s_{1m}, s_{3m}) or (e_{1m}, e_{3m}) of the stress or strain paths, calculated from contour integrals along it

$$s_{1m} = (1/p_s) \cdot \int s_1 \cdot |d\vec{s}'|, \quad s_{3m} = (1/p_s) \cdot \int s_3 \cdot |d\vec{s}'|, \quad p_s = \int |d\vec{s}'| \tag{4}$$

$$e_{1m} = (1/p_e) \cdot \int e_1 \cdot |d\vec{e}'|, \quad e_{3m} = (1/p_e) \cdot \int e_3 \cdot |d\vec{e}'|, \quad p_e = \int |d\vec{e}'| \tag{5}$$

where $|d\vec{s}'|$ and $|d\vec{e}'|$ are the lengths of infinitesimal segments of the stress and strain paths, while p_s and p_e are the respective path perimeters, see Fig. 1.

The MOI method calculates the path-equivalent range of a stress or strain path from the mass moment of inertia (MOI) of its corresponding unit-mass homogeneous wire. However, instead of using the axial MOI of the analogous wire, which is calculated about an *axis*, the Polar MOI (PMOI) is adopted instead, which represents the distribution of the wire (or load) path about a *single point*, its perimeter centroid. The PMOI of the stress or strain path about the perimeter centroid is then obtained from the contour integral of the square of the distance r_m between each point in the path and the path centroid, see Fig. 1, resulting in

$$I_p \equiv \frac{1}{p_s}\int \underbrace{\left[(s_1 - s_{1m})^2 + (s_3 - s_{3m})^2\right]}_{r_m^2} |d\vec{s}'| \;\text{ or }\; \frac{1}{p_e}\int \underbrace{\left[(e_1 - e_{1m})^2 + (e_3 - e_{3m})^2\right]}_{r_m^2} |d\vec{e}'| \tag{6}$$

The path-equivalent ranges are assumed proportional to the radius of gyration of the load path, which is equal to the square root of the PMOI of the unit-mass wire. This hypothesis is physically sound, since path segments of the load history further away from their mean components contribute more to the path-equivalent range, in the same way that wire segments further away from the perimeter centroid contribute more to the PMOI of an imaginary homogeneous wire. The path-equivalent stress and strain ranges become then

$$\Delta\sigma_{Mises} \;\text{ or }\; \Delta\varepsilon_{Mises} \cdot (1+\bar{\nu}) = \sqrt{12 \cdot I_p} \tag{7}$$

where the $\sqrt{12}$ term was calibrated to be consistent with the uniaxial case. The MOI method has been shown experimentally to effectively estimate path-equivalent ranges [2-3]. For convex stress or strain paths, it essentially reproduces the good predictions from the Maximum Rectangular Hull method [4].

The tension-torsion version or the 6D generalization of the MOI method can be directly used with invariant-based multiaxial fatigue damage models like Sines and Crossland. However, models based on stress or strain invariants like von Mises should not be used to make multiaxial fatigue damage predictions for directional-damage materials, like most metallic alloys, which fail due to a single dominant crack. For such materials, the MOI method needs to be applied to *projected* stress or strain paths, as discussed next.

MOI METHOD FOR THE CRITICAL-PLANE APPROACH

Most metallic alloys tend to initiate a single dominant microcrack under fatigue loadings. Under multiaxial loading conditions, this behavior tends to be better modeled by critical-plane fatigue-damage models, which search for the material plane at the critical point where the corresponding accumulated fatigue damage parameter is maximized, than by the simpler invariant-based models, which are direction independent. Multiaxial fatigue damage is then calculated in several candidate planes from their projected load histories, to find the critical plane where damage is maximized and thus where the microcrack is expected to initiate.

According to the critical-plane approach, the MOI method would lead to significant errors if directly applied to the original NP deviatoric histories, because the resulting ranges would be calculated on different planes at different points in time, not on the critical plane where the microcrack is expected to. So, instead of projecting the original 6D stress or strain history onto 5D deviatoric spaces, it should be projected onto the several candidate planes before proceeding with the fatigue damage analysis.

Although in general any plane can be a candidate at the critical point, Bannantine and Socie [5] narrowed down the search space for the critical plane at the critical point of the structural component when it is under free-surface conditions, as usual. They classified the most common microcracks into three types, which depend on the fatigue damage mechanism: Case A tensile or Case A shear microcracks, which grow at the critical point along planes perpendicular to the free surface; and Case B shear microcracks, which grow on planes that make an angle $\phi = 45^o$ with the free surface, see Fig. 2. To compact and hopefully clarify the critical plane notation in this work, Case A tensile planes are represented as A90(T), Case A shear as A90(S), and Case B shear as B45(S), where 90 or 45 come from their ϕ angles in degrees with respect to the free surface.

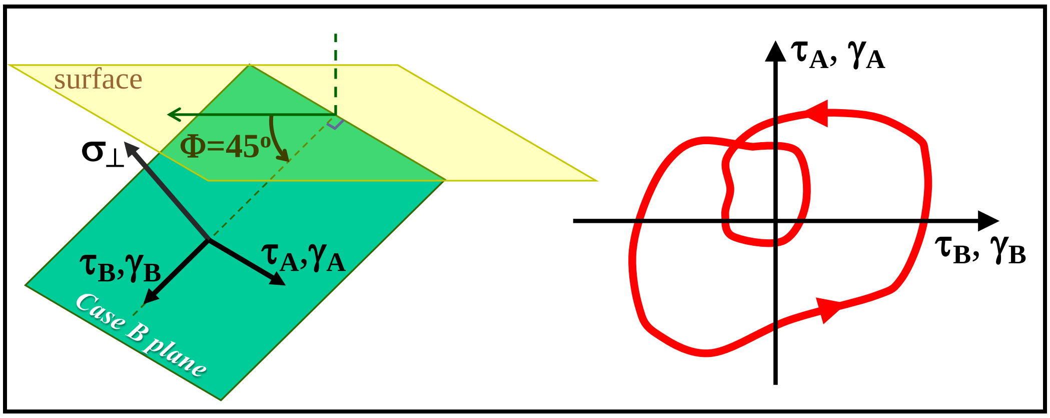

Fig. 2: NP shear strain path $\gamma_B \times \gamma_A$ (or shear stress path $\tau_B \times \tau_A$) acting on candidate planes at 45° from a free surface, for a general loading history.

A90(T) or A90(S) microcracks, which initiate perpendicular to the free surface, only involve one normal and one shear stress/strain component, so normal or shear ranges are quite easy to calculate under variable amplitude loading (VAL) conditions using classic uniaxial rainflow procedures. However, B45(S) microcracks involve in general two shear components, an in-plane stress τ_A (or strain γ_A) and an out-of-plane τ_B (or γ_B), see Fig. 2, which must be properly combined to evaluate their joint effect on fatigue damage.

The combination of both usually non-zero $\Delta\tau_B$ and $\Delta\tau_A$ ranges may cause the initiation of a combined Mode II-III B45(S) microcrack, with $\Delta\tau_B$ mainly contributing to increase its depth while $\Delta\tau_A$ is mainly tending to increase its width. The combination of $\Delta\tau_B$ and $\Delta\tau_A$ into an equivalent range $\Delta\tau$ is not a trivial step under general NP loadings, where the τ_B and the τ_A histories may be (and usually are) out of phase.

This process requires first a 2D rainflow algorithm such as the Modified Wang Brown method [6] to identify every load event from the $\tau_B \times \tau_A$ (or $\gamma_B \times \gamma_A$) history. Then, for each identified load event, its path segments are used to calculate a path-equivalent shear stress $\Delta\tau$ (or strain $\Delta\gamma$) range. The simplest approach for the $\tau_B \times \tau_A$ diagram is to assume a path-equivalent $\Delta\tau \equiv \sqrt{\Delta\tau_A^2 + \Delta\tau_B^2}$ for each identified load event, as discussed in [7]. However, this simple equivalent range expression would not be able to tell apart e.g. a rectangular from a less damaging cross-shaped $\tau_B \times \tau_A$ path with same $\Delta\tau_B$ and $\Delta\tau_A$, because both would wrongfully generate the same equivalent shear stress range $\Delta\tau$. Hence, this path-equivalent range is not a suitable solution to solve these problems in practical applications.

Another possible approach is to use the so-called convex-enclosure methods [1], which try to find circles, ellipses, or rectangles that circumscribe the load-event path in such 2D $\tau_B \times \tau_A$ or $\gamma_B \times \gamma_A$ diagrams. But convex-enclosure algorithms do not consider the actual shape of the loading path, usually failing when the load path shape is not convex.

This issue can be solved if the Moment-Of-Inertia (MOI) method is applied to the $\tau_B \times \tau_A$ (or $\gamma_B \times \gamma_A$) history projected on each B45 candidate plane, since it considers the influence of the load path shape, not only its convex enclosure. To do so, the load history of the two shear stresses or strains acting parallel to each B45 candidate plane first needs to be represented in a 2D $\tau_B \times \tau_A$ or $\gamma_B \times \gamma_A$ diagram, see Fig. 3, where a 2D rainflow followed by a 2D shear-shear version of the MOI method can be applied.

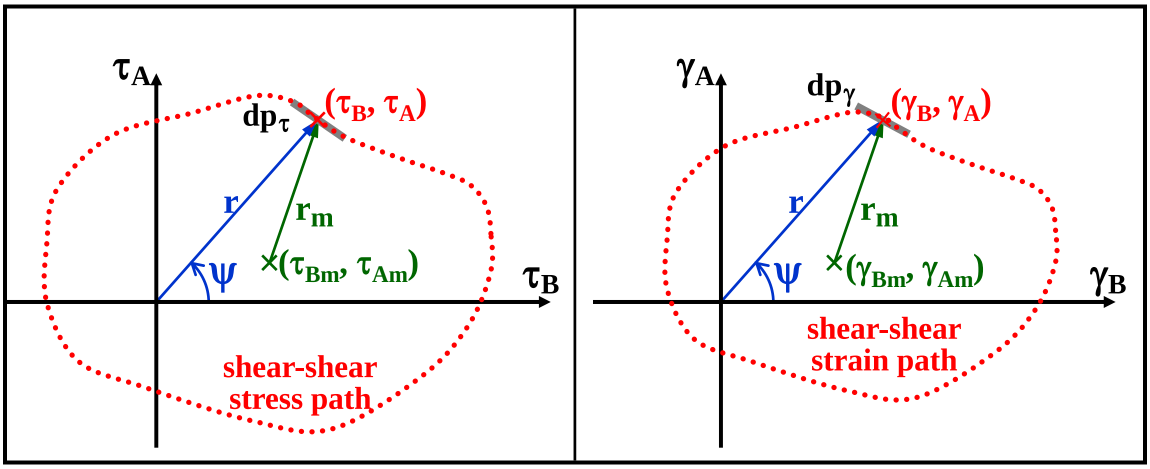

Fig. 3: Stress path of a 2D shear-shear history on a candidate plane (left) and corresponding strain path (right), both assumed as homogeneous wires with unit mass.

For each rainflow-counted path, the path perimeters p_τ or p_γ, the mean shear components (τ_{Bm}, τ_{Am}) or $(\gamma_{Bm}, \gamma_{Am})$, the associated PMOI I_p, and the resulting path-equivalent ranges $\Delta\tau$ and $\Delta\gamma$ from the MOI method become

$$p_\tau = \int \sqrt{d\tau_A^2 + d\tau_B^2}, \quad p_\gamma = \int \sqrt{d\gamma_A^2 + d\gamma_B^2} \tag{8}$$

$$\tau_{Bm} = (1/p_\tau) \cdot \int \tau_B \cdot \sqrt{d\tau_A^2 + d\tau_B^2}, \quad \tau_{Am} = (1/p_\tau) \cdot \int \tau_A \cdot \sqrt{d\tau_A^2 + d\tau_B^2} \tag{9}$$

$$\gamma_{Bm} = (1/p_\gamma) \cdot \int \gamma_B \cdot \sqrt{d\gamma_A^2 + d\gamma_B^2}, \quad \gamma_{Am} = (1/p_\gamma) \cdot \int \gamma_A \cdot \sqrt{d\gamma_A^2 + d\gamma_B^2} \tag{10}$$

$$\begin{aligned} I_p &\equiv \frac{1}{p_\tau} \cdot \int \left[(\tau_B - \tau_{Bm})^2 + (\tau_A - \tau_{Am})^2 \right] \cdot \sqrt{d\tau_A^2 + d\tau_B^2} \quad \text{or} \\ I_p &\equiv \frac{1}{p_\gamma} \cdot \int \left[(\gamma_B - \gamma_{Bm})^2 + (\gamma_A - \gamma_{Am})^2 \right] \cdot \sqrt{d\gamma_A^2 + d\gamma_B^2} \end{aligned} \tag{11}$$

$$\Delta\tau \text{ or } \Delta\gamma = \sqrt{12 \cdot I_p} \tag{12}$$

The resulting ranges are then used in a shear-based multiaxial fatigue model together with Miner's rule to obtain the accumulated shear damage on each B45 candidate plane. The critical plane is then the one among all A90(T)/A90(S) and B45(S) planes that has the maximum accumulated damage. For further details, see [8].

CONCLUSIONS

In this work, strain-based versions of the Moment Of Inertia (MOI) method were presented to allow the calculation of path-equivalent strain ranges under low cycle fatigue conditions. A critical-plane version of the MOI method was also presented, applicable for materials that fail due to a single dominant crack, like most metallic alloys. The combination of both out-of-plane γ_B and in-plane γ_A shear components into an equivalent strain range $\Delta\gamma$ is fundamental to correctly account for shear damage on candidate planes inclined at 45^o from the free surface. The MOI method is robust, computationally inexpensive and physically sound, since load paths with larger amplitudes are intrinsically associated with wider wires with increased MOI. Moreover, it deals with non-convex load paths better than convex-enclosure methods, since it accounts for the contribution of every single segment of the path. It thus deals with arbitrarily shaped multiaxial load histories without losing information about such shapes, while its different versions make it applicable for both invariant-based and critical-plane approaches.

REFERENCES

[1] Meggiolaro, M.A.; Castro, J.T.P.:
An improved multiaxial rainflow algorithm for nonproportional stress or strain histories - Part I: enclosing surface methods
Int J Fatigue 42 (2012), pp. 217-226

[2] Meggiolaro, M.A.; Castro, J.T.P.:
The moment of inertia method to calculate equivalent ranges in non-proportional tension–torsion histories
J. Mat. Res. Tech. 4 (2015) 229-234

[3] Meggiolaro, M.A.; Castro, J.T.P.; Wu, H.:
On the use of tensor paths to estimate the non-proportionality factor of multiaxial stress or strain histories under free-surface conditions
Acta Mechanica 227 (2016), pp. 3087-3100

[4] Araújo, J.A.; Dantas, A.P.; Castro, F.C.; Mamiya, E.N.; Ferreira, J.L.A.:
On the characterization of the critical plane with a simple and fast alternative measure of the shear stress amplitude in multiaxial fatigue
Int. J. Fatigue 33 (2011) 1092-1100

[5] Bannantine, J.A.; Socie, D.F.:
A variable amplitude multiaxial fatigue life prediction method
In: K.F. Kussmaul, D.L. McDiarmid, D.F. Socie (Eds.), Fatigue under Biaxial and Multiaxial Loading, ESIS Publication 10 (1991), pp. 35-51

[6] Meggiolaro, M.A.; Castro, J.T.P.:
An improved multiaxial rainflow algorithm for non-proportional stress or strain histories – Part II: The Modified Wang–Brown method
Int. J. Fatigue 42 (2012), pp. 194-206

[7] Castro, F.C.; Araújo, J.A.; Mamiya, E.N.; Pinheiro, P.A.:
Combined resolved shear stresses as an alternative to enclosing geometrical objects as a measure of shear stress amplitude in critical plane approaches
Int. J. Fatigue 66 (2014), pp. 161-167

[8] Castro, J.T.P.; Meggiolaro, M.A.:
Fatigue Design Techniques, Volume 2: Low-Cycle and Multiaxial Fatigue.
CreateSpace (2016)

Corresponding author: meggi@puc-rio.br